

Role of three-dimensional imaging integration in atrial fibrillation ablation

Roberto De Ponti, Raffaella Marazzi, Domenico Lumia, Giuseppe Picciolo, Roberto Biddau, Carlo Fugazzola, Jorge A Salerno-Uriarte

Roberto De Ponti, Raffaella Marazzi, Giuseppe Picciolo, Roberto Biddau, Jorge A Salerno-Uriarte, Department of Heart, Brain and Vessels, Ospedale di Circolo e Fondazione Macchi, University of Insubria, IT-21100 Varese, Italy

Domenico Lumia, Carlo Fugazzola, Department of Radiology, Ospedale di Circolo e Fondazione Macchi, University of Insubria, IT-21100 Varese, Italy

Author contributions: All authors equally contributed to this paper.

Correspondence to: Roberto De Ponti, MD, FHRS, Department of Heart, Brain and Vessels, Ospedale di Circolo e Fondazione Macchi, University of Insubria, Viale Borri, 57, IT-21100 Varese, Italy. rdeponti@alice.it

Telephone: +39-332-278934 Fax: +39-332-393644

Received: June 17, 2010 Revised: July 13, 2010

Accepted: July 20, 2010

Published online: August 26, 2010

© 2010 Baishideng. All rights reserved.

Key words: Catheter ablation; Atrial fibrillation; Electro-anatomic mapping; Multislice computed tomography; Magnetic resonance imaging

Peer reviewers: Salah AM Said, MD, Department of Cardiology, Geerdinksweg 141, 7555 DL Hengelo, The Netherlands; Mien-Cheng Chen, MD, Professor of Medicine, Division of Cardiology, Department of Internal Medicine, Chang Gung Memorial Hospital-Kaohsiung Medical Center, Chang Gung University College of Medicine, Kaohsiung, 123, Ta Pei Road, Niao Sung Hsiang, Kaohsiung Hsien 83301, Taiwan, China

De Ponti R, Marazzi R, Lumia D, Picciolo G, Biddau R, Fugazzola C, Salerno-Uriarte JA. Role of three-dimensional imaging integration in atrial fibrillation ablation. *World J Cardiol* 2010; 2(8): 215-222 Available from: URL: <http://www.wjgnet.com/1949-8462/full/v2/i8/215.htm> DOI: <http://dx.doi.org/10.4330/wjc.v2.i8.215>

Abstract

Atrial fibrillation is the most common arrhythmia and in symptomatic patients with a drug-refractory form, catheter ablation aimed at electrically disconnecting the pulmonary veins (PVs) has proved more effective than use of antiarrhythmic drugs in maintaining sinus rhythm during follow-up. On the other hand, this ablation procedure is complex, requires specific training and adequate clinical experience. A main challenge is represented by the need for accurate sequential positioning of the ablation catheter around each veno-atrial junction to deliver point-by-point radiofrequency energy applications in order to achieve complete and persistent electrical disconnection of the PVs. Imaging integration is a new technology that enables guidance during this procedure by showing a three-dimensional, pre-acquired computed tomography or magnetic resonance image and the relative real-time position of the ablation catheter on the screen of the electroanatomic system. Reports in the literature suggest that imaging integration provides accurate visual information with improvement in the procedure parameters and/or clinical outcomes of the procedure.

INTRODUCTION

Over the last decade, catheter ablation has been a treatment option increasingly offered to patients with symptomatic atrial fibrillation (AF) refractory to antiarrhythmic drug therapy. In the updated survey on catheter ablation for AF^[1], an almost 2-fold increase in the number of patients treated between 2003 and 2006 was observed as compared with the number between 1995 and 2002. In this survey, this treatment option shows to be effective in roughly 80% of patients after 1.3 procedures per patient, on average, with about 70% of the patients not requiring further antiarrhythmic drugs during a 10 ± 8 mo follow-up. These data are corroborated by the results of several, recently published meta-analyses on the efficacy of catheter ablation and of antiarrhythmic drug therapy for the prevention of AF^[2-5]. Particularly, the most updated

meta-analysis of randomized, controlled trials comparing antiarrhythmic drug therapy *vs* catheter ablation of AF^[5] showed that catheter ablation with isolation of the pulmonary veins (PVs) was associated with markedly increased odds of maintaining sinus rhythm as compared to antiarrhythmic drug therapy (77% *vs* 29%) in a patient population with predominantly paroxysmal AF (70%), refractory to 2 antiarrhythmic drugs with a mean left atrial diameter of 42 ± 3 mm. Moreover, a study performed in the United States^[6] using a simulation mode showed that catheter ablation of symptomatic, drug-refractory AF with or without continuation of antiarrhythmic drug therapy during follow up appeared reasonably cost-effective compared to antiarrhythmic drug therapy alone, based on improved quality of life and avoidance of future health care costs.

In the past, different techniques and tools for catheter ablation of the PVs in patients with AF have been proposed and used. More recently, the HRS/EHRA/ECAS expert consensus statement^[7] underlined that ablation of PVs with demonstration of complete electrical isolation is the cornerstone for most AF ablation procedures. Furthermore, this document stated that careful identification of the PV ostia is mandatory to avoid ablation within the PVs, which carries a significant risk of PV stenosis, which is a severe complication. Therefore, it appears mandatory that the operator should use an appropriate technology to identify the PV ostia and, more importantly, the real-time relative position of the ablation catheter.

In this review, the rationale, methods, and results of using electroanatomic mapping with imaging integration to orient catheter ablation of AF aimed at electrical disconnection of the PVs will be described in detail.

RATIONAL FOR USING ELECTROANATOMIC MAPPING WITH IMAGING INTEGRATION

Initially, to visualize the PVs during the AF ablation procedure, two methods have been reported: PV angiography and intracardiac echography. When these methods are used, different techniques and tools can be utilized to improve the quality of visualization of PV anatomy during the AF ablation procedure^[7]. However, these techniques provide two-dimensional images, sometimes with suboptimal resolution and, in the case of intracardiac echography, it requires extra costs, dedicated access and personnel. Moreover, the PVs anatomy in terms of number and morphology of oses, branching and supernumerary PVs is very individual, as already reported^[8-11]. This anatomic variability may influence both success and safety of the procedure, if the PV os/antrum is not adequately visualized during the procedure. In fact, if the presence of supernumerary veins is not recognized and their os not treated, the success rate can be suboptimal^[7,12]. On the other hand, the ablation performed inside the PV due to

Table 1 Anatomic variants of the pulmonary veins in 147 consecutive patients with atrial fibrillation undergoing a 64-slice computed tomography scan the day before the ablation procedure

Anatomy	n (%)
Four distinct PV oses	81 (55)
Common os	66 (45)
Left PVs	55
Right PVs	7
Left and right PVs	1
Inferior PVs	3
Adjunctive PVs	21 (14)
Right	16
Left	2 ¹
Roof	4

¹1 patient showed an adjunctive pulmonary vein both right and left. PV: Pulmonary vein.

mislocalization of the true ostium may affect both the complication rate, since the risk of PV stenosis may increase significantly, and the success rate, since proximal PV foci can be left untreated.

Based on these considerations and the experience accumulated in several centers over recent years, the best way to visualize the individual variants of PVs is three-dimensional imaging, which can be obtained before the procedure, by computed tomography (CT) scanning or magnetic resonance imaging (MRI), or during the procedure, by three-dimensional rotational angiography^[13]. The latter technology provides on-line intraprocedure angiographic data of the left atrium (LA) and PVs but, so far, its availability is limited. Therefore, the most frequently used technique is CT or MRI scan of the LA and PVs, which is acquired off-line, usually the day before the procedure. MRI avoids radiation exposure, but it might be tolerated less well, especially by claustrophobic patients, and the three-dimensional rendering might be operator-dependent. On the other hand, CT obviously implies radiation exposure, which depends on the method used for imaging acquisition.

Our personal experience in 147 consecutive patients with AF undergoing a 64-slice CT scan for imaging of the LA and the PVs the day before the ablation procedure shows high individual variability, including rare forms of anatomic variants (Table 1). As shown, the most expected anatomy with four separated PV oses is observed in only 55% of the patients and in 14% of cases adjunctive PVs are present, with an os close to the right or left PVs, but independently draining or, more peculiarly, located in the medial roof of the LA. The finding of a common trunk is by far more frequently observed in the left PVs. Interestingly, the already described^[14-17] presence of a common os of the left and right inferior PVs, although rare (2%), significantly distorts the LA anatomy (Figure 1). In this patient population, the radiation exposure was very much dependent on the acquisition technique. In fact, the radiation

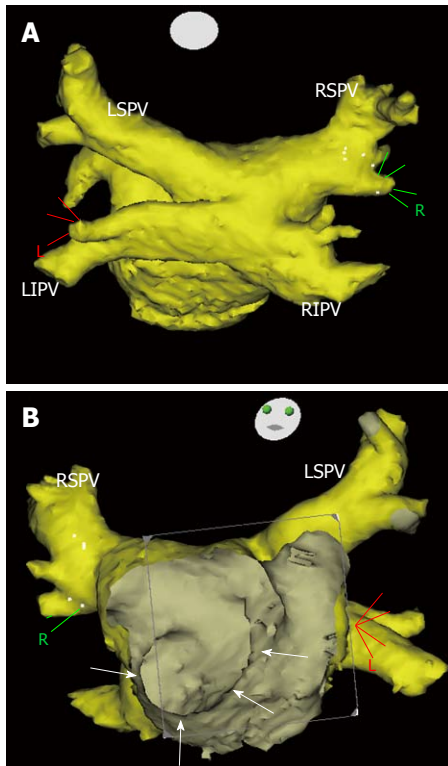


Figure 1 Three dimensional computed tomography image of a peculiar anatomic variant of the pulmonary veins in a patient with atrial fibrillation and no structural heart disease. A: The postero-anterior view of the left atrium and pulmonary veins; B: The endocardial aspect of the pulmonary vein oses after removal of the anterior wall of the left atrium. The common os of the left and right inferior pulmonary veins is evident both on the epicardial and endocardial (arrows) aspects. The oses of the right and left superior pulmonary veins are adjacent and more anterior, to the common os. LIPV: Left inferior pulmonary vein; LSPV: Left superior pulmonary vein; RIPV: Right inferior pulmonary vein; RSPV: Right superior pulmonary vein.

exposure was 7.6-fold higher in the first 30 patients, in whom the CT scan was performed in ECG-gated mode, as compared to the following patients, scanned in a non ECG-gated mode [23 ± 8 mSv (range 9.7-44 mSv) *vs* 3 ± 1 mSv (range 0.9-5.7 mSv), respectively, $P < 0.0001$].

The high resolution anatomical information provided by three-dimensional preprocedure imaging can be useful to the operator before the procedure. However, the best use of this imaging is obtained when, during the procedure, they are imported and integrated in the electroanatomic mapping, so that on the system screen the icon of the ablation catheter is visualized in real-time, with due accuracy, on the high resolution image of the PV os/antrum. In this way, it is possible to both accurately establish where the ablation lesion is performed and to manipulate the ablation catheter around the PV os with minimal or no use of fluoroscopy.

METHODS FOR ACCURATE IMAGING INTEGRATION OF THE LA AND PVS

For the purpose of better understanding the integration

process, it can be subdivided in four different steps. First, the CT or MRI pre-acquired data set is imported in the electroanatomic system and it is “segmented” using dedicated software, so that the three-dimensional rendering of the LA and PVs is extracted. This image can be evaluated both from the epicardial and endocardial aspect, as shown in Figure 1. Second, at the beginning of the procedure, after transeptal catheterization has been accomplished, the LA is electroanatomically reconstructed by acquiring a variable number of points in this heart chamber. The third step is represented by the “registration” phase. One or more pairs of landmarks, each one positioned on the electroanatomic map and on the assumed corresponding site of the CT/MRI surface, are identified. Usually, sites easy to identify are used for this purpose (e.g. left atrial roof and os of the PVs). Then using the “landmark registration” and the “surface registration” options, each landmark on the two surfaces is superimposed and the two surfaces are superimposed as well, in such a way that the best match between the two images is obtained. In the fourth and last step, the accuracy of the superimposition of the two surfaces is checked. If imaging integration was performed accurately, the icon of the mapping/ablation catheter, visualized in real-time on the screen of the electroanatomic system, can be navigated in the high resolution anatomy image provided by the CT/MRI with optimal accuracy of localization.

As reported in Table 2, several published studies have mainly focused on the methods to integrate the CT or MRI images of the LA/PVs into an electroanatomic system and to evaluate the accuracy of this process. Overall, these studies have included more than 500 patients with a variable proportion of patients with paroxysmal AF, ranging from 31% to 83%. The CartoMerge technology and 64-slice CT have been used in the vast majority of the studies as an electroanatomic system and preprocedure three-dimensional imaging modality, respectively. Intra-cardiac echocardiography has been also sparingly used. In almost all cases, using the electroanatomic system, the LA and the oses of the PVs have been reconstructed as a single chamber and the number of acquired sites to reconstruct these anatomical structures varied in different studies, from 224 ± 59 to 24 ± 7 sites. Generally, all the studies reported that the integration process was successful in the majority of patients, so that the mapping/ablation catheter could be reliably navigated in the imported three-dimensional rendering of CT or MRI. The accuracy of the integration process has been evaluated by the distance between an electroanatomic point and the correspondent point on the CT/MRI, which is automatically given by the system. This value represents the average error, being the distance between the site where the catheter is shown to be on the CT/MRI image and the site where it actually is. In these reports, this value varied from 2.9 ± 0.7 mm to 1.4 ± 0.3 mm, on average, which confirms an accurate and clinically useful integration process since the catheter tip is 3.5 mm in length and every distance below

Table 2 Overview of the studies designed to evaluate the methods and accuracy of imaging integration of the left atrium/pulmonary veins in an electroanatomic mapping system during the atrial fibrillation ablation procedure

Author	No. of pts	Percentage of pts with parox. AF	System	3D-imaging (No. of pts)	ICE	Type of EA reconstruction: single/multi chamber	No. of EA points	Distance between EA and CT/MRI points (mm)		
								Mean	Maximum	Minimum
Tops <i>et al</i> ^[18]	16	31	CartoMerge	64-slice CT	N	Single	224 ± 59	2.1 ± 0.2	2.8 ± 1.8	1.7 ± 1.2
Dong <i>et al</i> ^[19]	16	62	CartoMerge	MRI (8)/ 64-slice CT (8)	N	Single	24 ± 7	2.1 ± 0.5	2.7 ± 1.8	0.9 ± 0.8
Kistler <i>et al</i> ^[20]	30	40	CartoMerge	8-slice CT	N	Single	39 ± 8	2.3 ± 0.4	9.3 ± 2.4	0 ± 0
Martinek <i>et al</i> ^[21]	40	65	CartoMerge	16-slice CT	N	Single	63 ± 14	1.6 ± 1.2	N/A	N/A
Heist <i>et al</i> ^[22]	61	57	CartoMerge	MRI (50)/ 64-slice CT (11)	N	Multi (LA + Ao)	LA (49 ± 25) Ao (148 ± 41)	1.9 ± 0.6	4.3 ± 3.4	1.2 ± 1.0
Fahmy <i>et al</i> ^[23]	124	55	CartoMerge	64-slice CT	N	N/A	59 ± 22	2.2 ± 1.7	N/A	N/A
Daccarett <i>et al</i> ^[24]	18	58	CartoMerge	64-slice CT	Y	Single	41 ± 8	5-10 ¹	N/A	N/A
Bertaglia <i>et al</i> ^[25]	40	55	CartoMerge	MRI	N	Single	37 ± 10	1.3 ± 1.0	N/A	N/A
Richmond <i>et al</i> ^[26]	23	61	NAVx Fusion	8-slice CT	N	Single	N/A	3.2 ± 0.9	6.1 ± 1.0	2.9 ± 0.7
Brooks <i>et al</i> ^[27]	55	53	NAVx Fusion	64-slice CT	N	Single	N/A	2.6 ± 2.2	6.6 ± 2.8	1.9 ± 0.4
Rossillo <i>et al</i> ^[28]	40	45	CartoMerge	Multislice CT	Y	Single	47 ± 9	1.4 ± 0.3	N/A	N/A
Nölker <i>et al</i> ^[29]	38	50	CartoMerge	Rotational angiography	N	Single	104 ± 59	2.2 ± 0.4	N/A	N/A
Ejima <i>et al</i> ^[30]	24	83	CartoMerge	64-slice CT	N	Single	88 ± 34	1.7 ± 0.5	6.1 ± 2.7	0.04 ± 0.03

¹Distance between an electroanatomic (EA) point and the same point localized by ICE. 3D: Three dimensional; AF: Atrial fibrillation; Ao: Aorta; CT: Computed tomography; ICE: Intra-cardiac echocardiography; LA: Left atrium; MRI: Magnetic resonance imaging; N: No; Y: Yes; N/A: Not available; Parox.: Paroxysmal; pts: Patients.

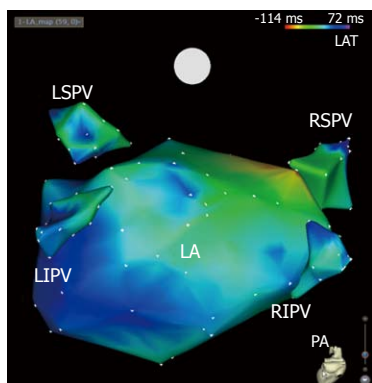


Figure 2 Postero-anterior view of the electroanatomic activation mapping of the left atrium and pulmonary veins. These have been reconstructed as five separate chambers using the Carto system and acquiring a few sites while the mapping catheter is manipulated in these anatomic structures. Colors indicate the activation sequence from the earliest in red (antero-medial part of the left atrium) to the latest in dark blue (postero-lateral part of the left atrium and distal part of the pulmonary veins). LA: Left atrium; LIPV: Left inferior pulmonary vein; LSPV: Left superior pulmonary vein; RIPV: Right inferior pulmonary vein; RSPV: Right superior pulmonary vein.

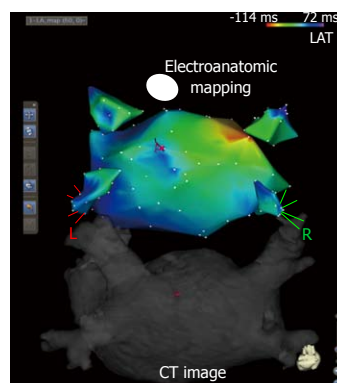


Figure 3 Postero-anterior view of the electroanatomic map shown in Figure 2 and of the three-dimensional rendering of the computed tomography scan, both in a postero-anterior view. A couple of points (small red flags on the electroanatomic mapping and computed tomography) have been identified on the left atrial roof. These two landmarks will be used to initially guide the superimposition of the two surfaces. CT: Computed tomography.

this value can be considered, with the due precautions, as acceptable.

In our experience, the method to integrate a 64-slice CT image (Aquilion 64, Toshiba Medical Systems, Tokyo, Japan) of the LA and PVs is slightly different from what has been reported in other studies. Briefly, after transseptal catheterization has been accomplished, the LA and the PVs are electroanatomically reconstructed by using the Carto 3 electroanatomic mapping system (Biosense-Webster, Diamond Bar, CA, USA) as five separate chambers, shown in Figure 2. On average, 40 sites in the body of the LA are acquired, while 20 sites

and 15 sites in the proximal part of the superior and inferior PVs, respectively, are also acquired. Generally, the acquired sites are homogeneously distributed in the chamber and particular care is taken when points are acquired in the PVs, so that catheter manipulation does not distort the PV anatomy. Subsequently, as shown in Figure 3, a single site in the left atrial roof is identified, both on the CT image and the electroanatomic mapping to serve as the landmark for the first raw superimposition of the two surfaces. Afterwards, superimposition is improved by the “surface registration” option, which finds the best match between the electroanatomic maps and the CT images by rotating the two surfaces relatively. Then, an accuracy check is performed by evaluating the

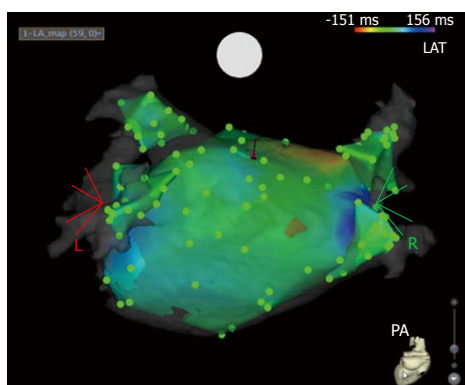


Figure 4 The two surfaces have been superimposed based on the guide provided by the two landmarks. The match of the two surfaces has been further improved with the so-called “surface registration” option, obtaining optimal integration. The accuracy of this process is then checked by verifying the distance between each electroanatomic point and the corresponding site on the computed tomography surface. In this case, all sites in the electroanatomic maps are marked by a green dot, which identifies the distance between the two surfaces as < 5 mm.

distance of each electroanatomic point from the corresponding site on the CT image. As shown in Figure 4, this can be done simply by using the software option that identifies sites with a distance < 5 mm as green dots, sites with a distance between 5 mm and 10 mm as yellow dots and sites with a distance > 10 mm as red dots. Therefore, during this final phase, sites with a distance > 5 mm should be deleted, while the catheter, visualized in real-time as an icon on the system screen, is moved in the LA and especially around the PV os/antrum to check the concordance between the actual catheter position and its display on the CT image. During this phase, other sites can be acquired to improve the quality of the integration. After the integration process has been concluded, the electroanatomic maps of the LA and PVs become transparent and the operator can manipulate the catheter looking at the projection of the catheter icon on the epicardial and endocardial aspect of the CT image, with minimal or no use of fluoroscopy, to deploy sequential radiofrequency energy lesions around the PV oses (Figure 5). In our institution, the accuracy of this integration process has been carefully evaluated in 150 consecutive patients undergoing catheter ablation of AF with electrical disconnection of the PVs. For this purpose, the distance between the actual site of radiofrequency energy application, based on different parameters (electrical signal, PV angiography, value of impedance, and three-dimensional imaging) and the corresponding site at the PV os on the CT imaging was calculated. The accuracy of integration has been defined as optimal if this distance was < 2 mm, acceptable if between 2 and 5 mm and unacceptable if > 5 mm. In this patient series, the accuracy was evaluated along the perimeter of 532 junctions between the PV and LA; in 68 patients a common os was found. An optimal imaging integration was observed in 75% of the PV-LA junctions, while it was acceptable in 16% and unacceptable in only 9%. Thus, manipulation of the ablation catheter around

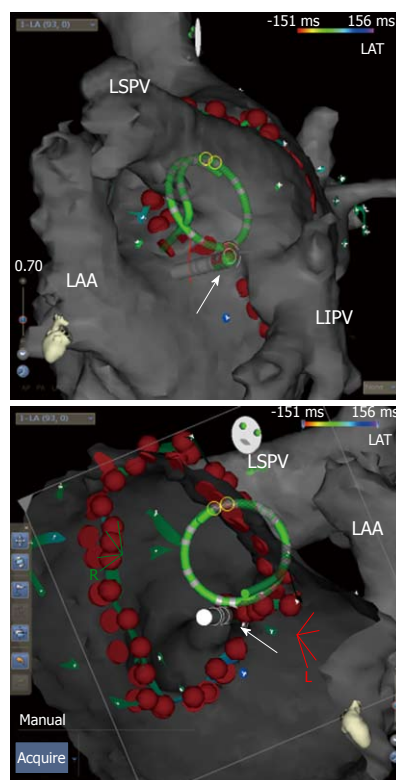


Figure 5 After completing the imaging integration process, pulmonary vein ablation is initiated. The screen of the electroanatomic system shows simultaneously the epicardial (upper) and endocardial (down) aspects of the high resolution computed tomography image of the common os of the left pulmonary veins present in this patient. The green circular icon identifies the multipolar circular mapping catheter, positioned inside the common os to verify its electrical disconnection. The icon of the ablation catheter (white arrows) is also visible, so that this catheter can be manipulated to navigate the three-dimensional computed tomography image with minimal or no use of fluoroscopy. Each red dot marks the site where radiofrequency energy has been applied along the venoatrial junction of the left pulmonary veins to achieve their electrical disconnection. LIPV: Left inferior pulmonary vein; LSPV: Left superior pulmonary vein; LAA: Left atrial appendage.

the os of the PVs to place radiofrequency energy applications with no or minimal use of fluoroscopy was done in 91% of the cases. Both in our experience, as well as in other centers' experiences^[20,21], the accuracy of integration was not affected by the difference of cardiac rhythm (sinus *vs* AF) during which the CT and the electroanatomic mapping were acquired. This is crucial, since the two images are acquired on two different days and it is likely that these patients exhibited different cardiac rhythms from 1 d to another. In fact, only 95/150 (63%) patients in our series were on the same cardiac rhythm (sinus rhythm or AF) during both (CT scan and electroanatomic mapping) imaging acquisition. In our experience, other factors that did not affect the accuracy of imaging integration were: mode of CT acquisition (ECG-gated *vs* non ECG-gated), left atrial volume, number of acquired sites in the LA and PVs and positioning of the multipolar circular mapping catheter to evaluate PV potentials during ablation. On the other hand, movements or respiratory artifacts during CT acquisition significantly altered the

Table 3 Overview of the studies designed to evaluate the impact of imaging integration for atrial fibrillation ablation on the procedure and clinical outcomes

Author	No. of pts	Type of study	Imaging	Type of evaluation	FU	Effect of imaging integration			
						Fluoroscopy time	Procedure duration	Complications	Clinical outcome
Kistler <i>et al</i> ^[31]	94	Non-randomized	CT	3D <i>vs</i> Merge	6 mo	↓	=	=	↑
Martinek <i>et al</i> ^[32]	100	Non-randomized	CT	XP <i>vs</i> Merge	6 mo	=	=	↓	↑
Kistler <i>et al</i> ^[33]	80	Randomized	CT	XP <i>vs</i> Merge	1 yr	=	=	=	=
Tang <i>et al</i> ^[34]	81	Randomized	CT	XP <i>vs</i> Merge	1 yr	↓	↓	=	=
Della Bella <i>et al</i> ^[35]	290	Randomized	CT	Conv <i>vs</i> Merge	> 1 yr	↑	↑	=	↑
Bertaglia <i>et al</i> ^[36]	573	Non-randomized	CT/MRI	Conv <i>vs</i> XP <i>vs</i> Merge	> 1 yr	=	↓	=	↑
Caponi <i>et al</i> ^[37]	299	Randomized	MRI	XP <i>vs</i> Merge	1 yr	↓	=	=	=

3D: Three-dimensional; Conv: Conventional; CT: Computed tomography; FU: Follow-up; Merge: CartoMerge; MRI: Magnetic resonance imaging; XP: Carto XP; ↑: Increased; ↓: Decreased; =: No difference; pts: Patients.

PV/left atrial geometry, therefore affecting the quality of imaging integration. In our experience, the quality of imaging integration was poor in a small percentage of cases (less than 10% of the PV oses), however, since quality greatly depends on respiratory or movement artifacts, great care should be taken during CT scan acquisition.

RESULTS OF IMAGING INTEGRATION IN TERM OF CLINICAL IMPACT

Using imaging integration to support AF ablation, the most important issue is whether this highly technological approach results in an improvement of the procedure parameters and the clinical outcome. Table 3 shows an overview of the results of the studies undertaken to assess the clinical usefulness of this technology^[31-37]. As shown, there are three non-randomized and four randomized studies published to date. While in the early reports the number of patients included was around 100, the 2009 multicentre Italian registry^[36] reported on more than 500 patients. In these studies, as well as in the studies aimed at assessing imaging integration accuracy, the most frequently used three-dimensional imaging modality was CT; the postablation follow-up was at least 1 year in most of the studies. In 5 of 7 studies^[31-34,37], the impact of imaging integration was compared with the use of three-dimensional mapping without imaging integration, whereas in the two remaining studies^[35,36], a comparison with the conventional technique (based only on fluoroscopy and the use of a circular mapping catheter) was made. It is evident that, apart from one study^[33], all the others reported significant improvement of procedure parameters and/or clinical outcome. Specifically, the two studies^[35,36] that compared imaging integration *vs* conventionally performed AF ablation reported improvement of clinical outcome with lower arrhythmia recurrences in the imaging integration group during follow-up. Among the other studies that compared an electroanatomic system with and without imaging integration, only two reported^[31,32] improvement in clinical outcome. However, of the 3 remaining studies, 2 reported improvement of the procedure

parameters with reduction of fluoroscopy^[34,37] and procedural time^[34].

Apart from the Italian registry^[36], which was a non-randomized study, all the other data are from single experiences. Indeed, the best results in term of evaluation of the clinical impact of imaging integration should be obtained by multicentre randomized studies enrolling a large cohort of patients. However, such studies are difficult to design, are long-lasting and sensitive to multiple different variables in different centers and, therefore, they are at risk of being inconclusive. Data provided to date favor the use of imaging integration technology in a complex procedure, such as AF ablation, to improve the quality of patient care.

REFERENCES

- 1 **Cappato R**, Calkins H, Chen SA, Davies W, Iesaka Y, Kalman J, Kim YH, Klein G, Natale A, Packer D, Skanes A, Ambrogi F, Biganzoli E. Updated worldwide survey on the methods, efficacy, and safety of catheter ablation for human atrial fibrillation. *Circ Arrhythm Electrophysiol* 2010; **3**: 32-38
- 2 **Noheria A**, Kumar A, Wylie JV Jr, Josephson ME. Catheter ablation vs antiarrhythmic drug therapy for atrial fibrillation: a systematic review. *Arch Intern Med* 2008; **168**: 581-586
- 3 **Nair GM**, Nery PB, Diwakaramenon S, Healey JS, Connolly SJ, Morillo CA. A systematic review of randomized trials comparing radiofrequency ablation with antiarrhythmic medications in patients with atrial fibrillation. *J Cardiovasc Electrophysiol* 2009; **20**: 138-144
- 4 **Calkins H**, Reynolds MR, Spector P, Sondhi M, Xu Y, Martin A, Williams CJ, Sledge I. Treatment of atrial fibrillation with antiarrhythmic drugs or radiofrequency ablation: two systematic literature reviews and meta-analyses. *Circ Arrhythm Electrophysiol* 2009; **2**: 349-361
- 5 **Piccini JP**, Lopes RD, Kong MH, Hasselblad V, Jackson K, Al-Khatib SM. Pulmonary vein isolation for the maintenance of sinus rhythm in patients with atrial fibrillation: a meta-analysis of randomized, controlled trials. *Circ Arrhythm Electrophysiol* 2009; **2**: 626-633
- 6 **Reynolds MR**, Zimetbaum P, Josephson ME, Ellis E, Danilov T, Cohen DJ. Cost-effectiveness of radiofrequency catheter ablation compared with antiarrhythmic drug therapy for paroxysmal atrial fibrillation. *Circ Arrhythm Electrophysiol* 2009; **2**: 362-369
- 7 **Calkins H**, Brugada J, Packer DL, Cappato R, Chen SA, Cri-

- jns HJ, Damiano RJ Jr, Davies DW, Haines DE, Haissaguerre M, Iesaka Y, Jackman W, Jais P, Kottkamp H, Kuck KH, Lindsay BD, Marchlinski FE, McCarthy PM, Mont JL, Morady F, Nademanee K, Natale A, Pappone C, Prystowsky E, Raviele A, Ruskin JN, Shemin RJ. HRS/EHRA/ECAS expert Consensus Statement on catheter and surgical ablation of atrial fibrillation: recommendations for personnel, policy, procedures and follow-up. A report of the Heart Rhythm Society (HRS) Task Force on catheter and surgical ablation of atrial fibrillation. *Heart Rhythm* 2007; **4**: 816-861
- 8 **Kato R**, Lickfett L, Meininger G, Dickfeld T, Wu R, Juang G, Angkeow P, LaCorte J, Bluemke D, Berger R, Halperin HR, Calkins H. Pulmonary vein anatomy in patients undergoing catheter ablation of atrial fibrillation: lessons learned by use of magnetic resonance imaging. *Circulation* 2003; **107**: 2004-2010
 - 9 **Lickfett L**, Kato R, Tandri H, Jayam V, Vasamreddy CR, Dickfeld T, Lewalter T, Luderitz B, Berger R, Halperin H, Calkins H. Characterization of a new pulmonary vein variant using magnetic resonance angiography: incidence, imaging, and interventional implications of the "right top pulmonary vein". *J Cardiovasc Electrophysiol* 2004; **15**: 538-543
 - 10 **Cirillo S**, Bonamini R, Gaita F, Tosetti I, De Giuseppe M, Longo M, Bianchi F, Vivalda L, Regge D. Magnetic resonance angiography virtual endoscopy in the assessment of pulmonary veins before radiofrequency ablation procedures for atrial fibrillation. *Eur Radiol* 2004; **14**: 2053-2060
 - 11 **Benini K**, Marini M, Del Greco M, Nollo G, Manera V, Centonze M. Role of multidetector computed tomography in the anatomical definition of the left atrium-pulmonary vein complex in patients with atrial fibrillation. Personal experience and pictorial essay. *Radiol Med* 2008; **113**: 779-798
 - 12 **Tsao HM**, Wu MH, Yu WC, Tai CT, Lin YK, Hsieh MH, Ding YA, Chang MS, Chen SA. Role of right middle pulmonary vein in patients with paroxysmal atrial fibrillation. *J Cardiovasc Electrophysiol* 2001; **12**: 1353-1357
 - 13 **Orlov MV**. How to perform and interpret rotational angiography in the electrophysiology laboratory. *Heart Rhythm* 2009; **6**: 1830-1836
 - 14 **Dukkipati S**, Holmvang G, Scozzaro M, D'Avila A, Reddy VY, Mansour M. An unusual confluence of the inferior pulmonary veins in a patient undergoing catheter ablation for atrial fibrillation. *J Cardiovasc Electrophysiol* 2006; **17**: 1034
 - 15 **Sra J**, Malloy A, Shah H, Krum D. Common ostium of the inferior pulmonary veins in a patient undergoing left atrial ablation for atrial fibrillation. *J Interv Card Electrophysiol* 2006; **15**: 203
 - 16 **Marazzi R**, De Ponti R, Lumia D, Fugazzola C, Salerno-Uriarte JA. Common trunk of the inferior pulmonary veins: an unexpected anatomical variant detected before ablation by multi-slice computed tomography. *Europace* 2007; **9**: 121
 - 17 **Shapiro M**, Dodd JD, Brady TJ, Abbara S. Common pulmonary venous ostium of the right and left inferior pulmonary veins: an unusual pulmonary vein anomaly depicted with 64-slice cardiac computed tomography. *J Cardiovasc Electrophysiol* 2007; **18**: 110
 - 18 **Tops LF**, Bax JJ, Zeppenfeld K, Jongbloed MR, Lamb HJ, van der Wall EE, Schalij MJ. Fusion of multislice computed tomography imaging with three-dimensional electroanatomic mapping to guide radiofrequency catheter ablation procedures. *Heart Rhythm* 2005; **2**: 1076-1081
 - 19 **Dong J**, Dickfeld T, Dalal D, Cheema A, Vasamreddy CR, Henrikson CA, Marine JE, Halperin HR, Berger RD, Lima JA, Bluemke DA, Calkins H. Initial experience in the use of integrated electroanatomic mapping with three-dimensional MR/CT images to guide catheter ablation of atrial fibrillation. *J Cardiovasc Electrophysiol* 2006; **17**: 459-466
 - 20 **Kistler PM**, Earley MJ, Harris S, Abrams D, Ellis S, Sporton SC, Schilling RJ. Validation of three-dimensional cardiac im-
age integration: use of integrated CT image into electroanatomic mapping system to perform catheter ablation of atrial fibrillation. *J Cardiovasc Electrophysiol* 2006; **17**: 341-348
 - 21 **Martinek M**, Nesser HJ, Aichinger J, Boehm G, Purerfellner H. Accuracy of integration of multislice computed tomography imaging into three-dimensional electroanatomic mapping for real-time guided radiofrequency ablation of left atrial fibrillation-influence of heart rhythm and radiofrequency lesions. *J Interv Card Electrophysiol* 2006; **17**: 85-92
 - 22 **Heist EK**, Chevalier J, Holmvang G, Singh JP, Ellinor PT, Milan DJ, D'Avila A, Mela T, Ruskin JN, Mansour M. Factors affecting error in integration of electroanatomic mapping with CT and MR imaging during catheter ablation of atrial fibrillation. *J Interv Card Electrophysiol* 2006; **17**: 21-27
 - 23 **Fahmy TS**, Mlcochova H, Wazni OM, Patel D, Cihak R, Kanj M, Beheiry S, Burkhardt JD, Dressing T, Hao S, Tchou P, Kautzner J, Schweikert RA, Arruda M, Saliba W, Natale A. Intracardiac echo-guided image integration: optimizing strategies for registration. *J Cardiovasc Electrophysiol* 2007; **18**: 276-282
 - 24 **Daccarett M**, Segerson NM, Günther J, Nölker G, Gutleben K, Brachmann J, Marrouche NF. Blinded correlation study of three-dimensional electro-anatomical image integration and phased array intra-cardiac echocardiography for left atrial mapping. *Europace* 2007; **9**: 923-926
 - 25 **Bertaglia E**, Brandolino G, Zoppo F, Zerbo F, Pascotto P. Integration of three-dimensional left atrial magnetic resonance images into a real-time electroanatomic mapping system: validation of a registration method. *Pacing Clin Electrophysiol* 2008; **31**: 273-282
 - 26 **Richmond L**, Rajappan K, Voth E, Rangavajhala V, Earley MJ, Thomas G, Harris S, Sporton SC, Schilling RJ. Validation of computed tomography image integration into the EnSite NavX mapping system to perform catheter ablation of atrial fibrillation. *J Cardiovasc Electrophysiol* 2008; **19**: 821-827
 - 27 **Brooks AG**, Wilson L, Kuklik P, Stiles MK, John B, Shashidhar, Dimitri H, Lau DH, Roberts-Thomson RL, Wong CX, Young GD, Sanders P. Image integration using NavX Fusion: initial experience and validation. *Heart Rhythm* 2008; **5**: 526-535
 - 28 **Rossillo A**, Indiani S, Bonso A, Themistoclakis S, Corrado A, Raviele A. Novel ICE-guided registration strategy for integration of electroanatomical mapping with three-dimensional CT/MR images to guide catheter ablation of atrial fibrillation. *J Cardiovasc Electrophysiol* 2009; **20**: 374-378
 - 29 **Nölker G**, Asbach S, Gutleben KJ, Rittger H, Ritscher G, Brachmann J, Sinha AM. Image-integration of intraprocedural rotational angiography-based 3D reconstructions of left atrium and pulmonary veins into electroanatomical mapping: accuracy of a novel modality in atrial fibrillation ablation. *J Cardiovasc Electrophysiol* 2010; **21**: 278-283
 - 30 **Ejima K**, Shoda M, Yagishita D, Futagawa K, Yashiro B, Sato T, Manaka T, Nakajima T, Ohmori H, Hagiwara N. Image integration of three-dimensional cone-beam computed tomography angiogram into electroanatomical mapping system to guide catheter ablation of atrial fibrillation. *Europace* 2010; **12**: 45-51
 - 31 **Kistler PM**, Rajappan K, Jahngir M, Earley MJ, Harris S, Abrams D, Gupta D, Liew R, Ellis S, Sporton SC, Schilling RJ. The impact of CT image integration into an electroanatomic mapping system on clinical outcomes of catheter ablation of atrial fibrillation. *J Cardiovasc Electrophysiol* 2006; **17**: 1093-1101
 - 32 **Martinek M**, Nesser HJ, Aichinger J, Boehm G, Purerfellner H. Impact of integration of multislice computed tomography imaging into three-dimensional electroanatomic mapping on clinical outcomes, safety, and efficacy using radiofrequency ablation for atrial fibrillation. *Pacing Clin Electrophysiol* 2007; **30**: 1215-1223
 - 33 **Kistler PM**, Rajappan K, Harris S, Earley MJ, Richmond L,

- Sporton SC, Schilling RJ. The impact of image integration on catheter ablation of atrial fibrillation using electroanatomic mapping: a prospective randomized study. *Eur Heart J* 2008; **29**: 3029-3036
- 34 **Tang K**, Ma J, Zhang S, Zhang JY, Wei YD, Chen YQ, Yu XJ, Xu YW. A randomized prospective comparison of CartoMerge and CartoXP to guide circumferential pulmonary vein isolation for the treatment of paroxysmal atrial fibrillation. *Chin Med J (Engl)* 2008; **121**: 508-512
- 35 **Della Bella P**, Fassini G, Cireddu M, Riva S, Carbucicchio C, Giraldi F, Maccabelli G, Trevisi N, Moltrasio M, Pepi M, Galli CA, Andreini D, Ballerini G, Pontone G. Image integration-guided catheter ablation of atrial fibrillation: a prospective randomized study. *J Cardiovasc Electrophysiol* 2009; **20**: 258-265
- 36 **Bertaglia E**, Bella PD, Tondo C, Proclemer A, Bottoni N, De Ponti R, Landolina M, Bongiorno MG, Corò L, Stabile G, Dello Russo A, Verlato R, Mantica M, Zoppo F. Image integration increases efficacy of paroxysmal atrial fibrillation catheter ablation: results from the CartoMerge Italian Registry. *Europace* 2009; **11**: 1004-1010
- 37 **Caponi D**, Corleto A, Scaglione M, Blandino A, Biasco L, Cristoforetti Y, Cerrato N, Toso E, Morello M, Gaita F. Ablation of atrial fibrillation: does the addition of three-dimensional magnetic resonance imaging of the left atrium to electroanatomic mapping improve the clinical outcome?: a randomized comparison of Carto-Merge vs. Carto-XP three-dimensional mapping ablation in patients with paroxysmal and persistent atrial fibrillation. *Europace* 2010; **12**: 1098-1104

S- Editor Cheng JX L- Editor Lutze M E- Editor Zheng XM